

# Probabilistically Shaped 64-QAM Transmission via Distortion-aware Phase Retrieval

Hanzi Huang<sup>1,2</sup>, Haoshuo Chen<sup>1,\*</sup>, Peiji Song<sup>1</sup>, Cheng Guo<sup>1</sup>,  
Qi Gao<sup>2</sup>, Yetian Huang<sup>1,2</sup>, Nicolas K. Fontaine<sup>1</sup>, Mikael Mazur<sup>1</sup>,  
Lauren Dallachiesa<sup>1</sup>, Roland Ryf<sup>1</sup>, Zhengxuan Li<sup>2</sup>, and Yingxiong Song<sup>2</sup>

<sup>1</sup> Nokia Bell Labs, 600 Mountain Ave, Murray Hill, NJ 07974, USA

<sup>2</sup> Key Laboratory of Specialty Fiber Optics and Optical Access Networks, Shanghai University, 200444 Shanghai, China

\*haoshuo.chen@nokia-bell-labs.com

**Abstract:** We experimentally demonstrate 50-GBaud probabilistically shaped 64-QAM transmission with 5.6-bits/symbol entropy over 80-km SSMF using carrierless intensity-only detection via a distortion-aware phase retrieval receiver, resulting net capacity over 200 Gb/s. © 2024 The Author(s)

## 1. Introduction

Driven by the large-scale deployment of cloud service, artificial intelligence, and other network traffic-consuming applications, the demand for high-capacity data center interconnects stimulates the development of low-cost transceivers supporting data rates  $\geq 200$  Gb/s/ $\lambda$  across single-span standard single-mode fiber (SSMF) [1]. Conventional intensity-modulation (IM) and direct detection (DD) technology is facing a bottleneck to push the line rate beyond 200 Gb/s per lane for distances above 10 km, where chromatic dispersion causes considerable power fading impairments, due to its one-dimension modulation essence. In contrast, coherent technology modulates the light over its amplitude, phase, and polarization spaces to enable four-dimension modulation to support higher capacity. Whereas, the detection of coherent systems requires the signal light to interfere with a stable local oscillator light to measure its phase, which demands sophisticated mechanisms including wavelength control and alignment between the transmitter (Tx) and receiver (Rx). To enable a laser-free Rx, advanced DD systems inserting an optical carrier at the Tx-side have been proposed, such as the Kramers-Kronig Rx [2] and Stokes-vector Rx [3], which require a certain level of carrier-to-signal power ratio (CSPR) to ensure their detection capability.

To eliminate the necessity for any reference carrier and facilitate a seamless transition from DD towards coherent systems, phase retrieval (PR) reception has been proposed [4, 5]. This approach circumvents the need for any form of signal-carrier beating during its detection process. Figure 1(a) gives the schematic a space-time (ST) diversity PR Rx [6], which transfers the optical signal with an optical bandwidth of  $B$  into intensity waveforms with an electrical bandwidth of  $2B$ .  $D$  denotes the dispersion value of the dispersive element. Operator  $\mathbf{P}$ ,  $\mathbf{T}$ ,  $\mathbf{H}$  denote 1-by-3 power splitting, time delay, 3-by-3 spatial scrambling operations within the ST diversity tributary. In a PR Rx, the signal phase information is inferred from measured intensity waveforms—produced by signal-signal beating components at different projections—using an iterative field reconstruction algorithm, rather than being directly measured. Therefore, the Tx hardware structure of a PR-based system is identical to that of a standard coherent system, but the reception scheme is maintained in an intensity detection manner. This not only grants PR resilience against wavelength drift and laser phase noise [7], but also facilitates integration with silicon photonics [8]. Despite its merits in combining DD and coherent systems, the experimental transmission of a carrierless PR-based system at 200 Gb/s per lane is yet to be demonstrated. Part of the reason is that PR systems lack effective compensation techniques against complicated channel impairments. Recently, we introduced and experimentally demonstrated an estimation and compensation framework against various channel distortion effects based on a two-photodiode (PD)-based PR Rx [9]. Following this approach, this paper experimentally demonstrates 50-GBaud probabilistically shaped (PS) 64-quadrature amplitude modulation (QAM) transmission with entropy of 5.6 bits/symbol over 80-km SSMF via a distortion-aware PR Rx, resulting in net capacity of 208.85 Gb/s after considering 10% pilot symbol ratio and 19.02% forward error correction (FEC) overhead.

## 2. Distortion-aware Phase Retrieval

Figure 1(b) illustrates the schematic of the PR transmission system as well as the offline transceiver digital signal processing (DSP) procedures employed in the experiment. To identify the channel distortion, this PR scheme uses a training sequence as depicted in the frame structure in Fig. 1(c). The training sequence is placed at the start of a frame, with two segments of guard symbols placed beside the training sequence to prevent unknown mixing symbols from the payload section under channel conditions with memory. The guard symbol sequences can be derived as the cyclic prefix and postfix of the training sequence to make them follow the circular convolution. The pilot symbols are distributed across the payload section evenly to eliminate global phase ambiguity. The Rx DSP employs the pre-known training sequence to conduct dispersion estimation, time synchronization, and determine channel impairments during the training stage. Within the training stage, various channel impairments, including Tx (complex-valued, field-based) and Rx (real-valued, intensity-based) frequency response impairments, in-phase and quadrature (IQ)-dependent impairments (IQ power imbalance, time skew, and phase mismatch), and modulator nonlinearity are estimated by minimizing errors between the distorted forward propagated training sequence's

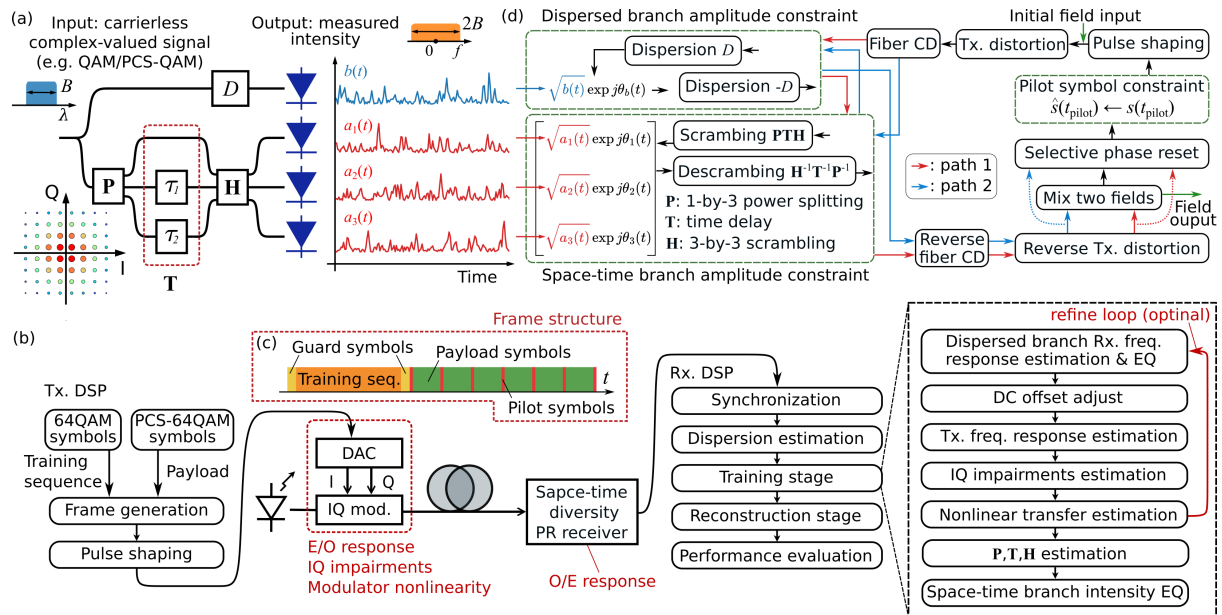


**Fig. 1:** Schematics of (a) a space-time diversity PR receiver, (b) the distortion-aware PR system with transceiver DSP flows and its (c) frame structure. (d) DSP procedures in the reconstruction stage.

intensity and the measured waveform of the dispersed tributary. Rx frequency response impairment is estimated and compensated by a feed-forward equalizer (FFE). A key concept to estimate the complex-valued Tx channel response is combining the distorted training sequence's phase with the measured amplitude to form an optical field estimation, and use that to conduct field-based channel estimation in an iterative manner. After completing a training cycle, the scheme offers an optional refinement loop to iteratively enhance estimation accuracy, as indicated by the red arrow in Fig. 1(b). Readers may refer to [9] for more detailed explanations. Then, the distorted optical field at Tx and its dispersed counterpart at Rx can be determined. The time delay, loss difference, and phase shift of the three branches in the ST diversity tributary are then estimated by minimizing the intensity error between the expected and measured intensities. The FFE-based intensity equalization can then be conducted by calculating the expected intensity waveforms of the ST branches. Figure 1(d) shows the DSP procedures of the reconstruction stage, which can be regarded as a modified Gerchberg-Saxton algorithm. The forward propagation resembles the real-world physical model of light propagation considering field-based Tx distortion. The backward propagation is the reverse of the light propagation process, where a reverse Tx distortion operation is added at the Tx projection plane. Besides, a dual-trace propagation mechanism is induced to enable higher accuracy and less likelihood of stagnation in local minima, as marked in red and blue arrows, which denote two estimated field traces experiencing amplitude constraints in different sequences.

### 3. Experimental Setup and Results

Figure 2 presents the experimental setup for transmitting 50-Gbaud PS 64-QAM signal over a SSF span of 80-km. At the transmitter side, a continuous wave (CW) laser with a linewidth of 10-kHz at 1531.1 nm is modulated by an IQ-Mach-Zehnder modulator (MZM) to produce the modulated signal with a roll-off factor of 1%. The training symbols consist of  $2^{13}$  uniform 64-QAM symbols, positioned between two guard symbol segments, each of which has a length of 64 symbols. The payload symbols contain  $2^{13}$  PS 64-QAM symbols repeating 30 times, which are generated by a Maxwell-Boltzmann distribution with entropy of 5.6 bits/symbol. The training symbols don't correlate with payload symbols and are re-scaled to maintain the same average power as the payload symbols. The output modulated signal is pre-amplified to -0.5 dBm by an erbium-doped fiber amplifier (EDFA) before launching into the 80-km SSF. A variable optical attenuator (VOA) is applied to adjust the received optical signal-to-noise ratio (OSNR) after transmission. At the Rx, another amplifier is used to re-boost the received optical power, with its output connected to a 99:1 splitter, with the 1% branch connected to an optical spectrum analyzer (OSA) for OSNR measurement. Inside the PR Rx, an optical band-pass filter (OBPF) is used to filter

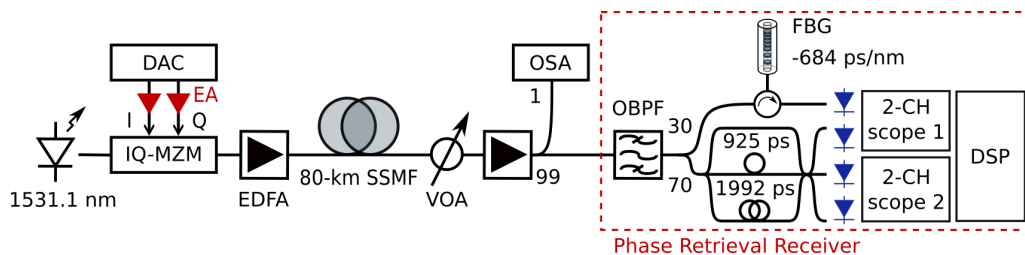


**Fig. 2:** Experimental setup for transmission over 80-km SSMF via the PR receiver.

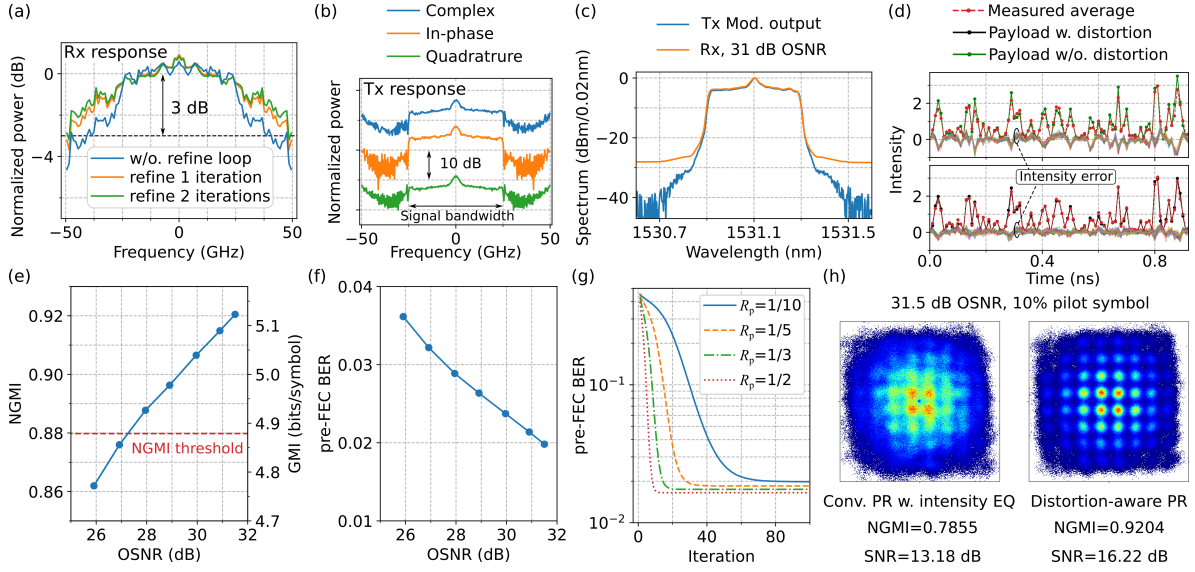


**Fig. 3:** Estimated (a) receiver- and (b) transmitter-side power frequency response. (c) Measured optical spectra. (d) Comparison between measured and estimated intensities with and without knowing channel distortion. Measured (e) NGMI, GMI and (f) BER curves versus OSNRs. (g) Measured BERs versus iteration number with different pilot symbol ratios. (h) Recovered constellation comparison.

out-of-band noise with a bandwidth of  $\sim 100$  GHz, cascaded by a 70:30 optical splitter. The dispersive element used in the PR Rx is a fiber Bragg grating (FBG)-based dispersion compensation module with a measured chromatic dispersion of  $-684$  ps/nm. The measured time delays of the ST tributary are 925 and 1992 ps compared with the shortest branch. The three ST branches' polarization states are manually aligned by polarization controllers, ensuring their complete interference. The received optical signals are detected by four 50-GHz photodiodes, and the detected electrical signals are captured by two digital storage oscilloscopes with a sampling rate of 160 GSa/s.

Figure 3(a) shows the estimated normalized Rx power frequency response with different refinement loop iterations. The Rx frequency response shows improvement with refinement iterations since the influence of Tx-related distortion is taken into account in the refinement loops. Figure 3(b) presents the estimated Tx power frequency response results with 2 refined loops. The curves representing in-phase, quadrature, and their merged complex channels are vertically shifted to show more clearly. The frequency response within signal bandwidth can be estimated and correlated to the measured spectra in Fig. 3(c), and out-of-band results are dominated by noise. Figure 3(d) compares approximation levels between the estimated and measured intensities for the dispersed branch, considering payload sequence with and without knowing the channel distortion knowledge. The intensity error traces for both schemes are calculated through 30 independent measurements and depicted using lines with different colors. Figure 3(e) shows the normalized generalized mutual information (NGMI) and generalized mutual information (GMI) results versus OSNR with 10% pilot symbol after 100 iterations, where a NGMI threshold of 0.8798 is given, corresponding to 19.02% FEC overhead [10, 11]. The pre-FEC bit error ratio (BER) results versus OSNR are also attached as a reference in Fig. 3(f). Figure 3(g) shows the pre-FEC BER results versus iteration number under different pilot symbol ratios  $R_p$ . It is shown that 10%  $R_p$  is sufficient for the algorithm to converge within 80 iterations and the converged BER does not significantly increase. Figure 3(h) compares the constellations of the recovered payload symbols, with NGMI and signal-to-noise ratio (SNR) results attached below. The distortion-aware PR shows a compact and clustered constellation, only with some phase ambiguity on the outer circle constellation points, which can be attributed to the intensity clipping effect during the analog-to-digital process. Despite this, its SNR reaches 16 dB, showing the robustness of distortion-aware PR against channel impairments during transmission. The net bit rate is  $50 \text{ GBaud} \times 0.9 \times [5.6 - 19.02\% / (1 + 19.02\%) \times 6] \text{ bits/symbol} = 208.85 \text{ Gbit/s}$  [12].

#### 4. Conclusions

We demonstrated 50-GBaud PS 64-QAM transmission with entropy of 5.6 bits/symbol over 80-km SSMF without resorting to any form of signal-carrier beating via a distortion-aware PR Rx, resulting in a net data rate over 200 Gb/s. As a dual-pol PR Rx directly supports polarization-division multiplexing transmission [4], there is potential to scale PR-based transmission for short-reach interconnection approaching  $400 \text{ Gb/s}/\lambda$ .

This work was supported in part by the National Key Research and Development Program of China (2021YFB2900801); Science and Technology Commission of Shanghai Municipality (22511100902, 22511100502); 111 project (D20031).

#### References

1. X. Zhou *et al.*, J. Lightw. Technol., 38(2), 475-484 (2020).
2. A. Mecozzi *et al.*, Optica, 3(11), 1220-1227 (2016).
3. D. Che *et al.*, J. Lightw. Technol., 33(3), 678-684 (2015).
4. H. Chen *et al.*, J. Lightw. Technol., 38(9), 2587-2597 (2020).
5. Y. Yoshida *et al.*, J. Lightw. Technol., 38(1), 90-100 (2020).
6. H. Chen *et al.*, Proc. OFC 2021, paper Th4D.3.
7. H. Chen *et al.*, Proc. ECOC 2021, paper Th3C1-PD2.1.
8. B. Stern *et al.*, Proc. ECOC 2023, paper M.A.2.2.
9. H. Huang *et al.*, arXiv:2310.05314.
10. J. Cho and L. Schmalen, Proc. ICC 2015, 4412-4417.
11. X. Chen *et al.*, Opt. Express, 27(21), 29916-29923 (2019).
12. F. Buchali *et al.*, J. Lightw. Technol., 34(7), 1599-1609 (2016).